Towards porous polymer monoliths for the efficient, retention-independent performance in the isocratic separation of small molecules by means of nano-liquid chromatography

Ivo Nischang*, Ian Teasdale, Oliver Brüggemann

Institute of Polymer Chemistry, Johannes Kepler University Linz, Welser Strasse 42, A-4060 Leonding, Austria

ABSTRACT

We have investigated the free-radical copolymerization dynamics of styrene and divinylbenzene in the presence of micro- and macro-porogenic diluents in 100 μm I.D. sized molds under conditions of slow thermal initiation leading to (macro)porous poly(styrene-*co*-divinylbenzene) monolithic scaffolds. These specifically designed experiments allowed the quantitative determination of monomer specific conversion against polymerization time to derive the porous polymer scaffold composition at each desirable copolymerization stage after phase separation. This was carried out over a time scale of 3 h up to 48 h polymerization time, enabling the efficient and repeatable termination of the polymerization reactions. In parallel, the porous and hydrodynamic properties of the derived monolithic columns were thoroughly studied in isocratic nano-LC mode for the reversed-phase separation of a homologous series of small retained molecules. At the optimized initiator concentration, polymerization temperature and time, the macroporous poly(styrene-*co*-divinylbenzene) monoliths show a permanent mesoporous pore space, which was readily observable by electron microscopy and indicated by nitrogen adsorption experiments. Under these conditions, we consistently find a polymer scaffold composition which suggests a high degree of cross-linking and thus minimum amount of gel porosity. These columns reveal a retention-insensitive plate height in the separation of small retained molecules which only slightly decreases at increased linear mobile phase velocity. As the polymerization progresses, a build-up of less-densely cross-linked material occurs, which is directly reflected in the observed consistent increase in retention and plate heights. This leads to a significant deterioration in overall isocratic separation performance. The decrease in performance is ascribed in particular to the increased mass transfer resistance governing the monoliths' performance over the whole linear chromatographic flow velocity range at polymerization times significantly higher than that of phase separation. The performance of the optimized monoliths only becomes limited by fluid dispersion due to the poorly structured macroporous pore space.

© 2010 Elsevier B.V. All rights reserved.

1. Introduction

Monolithic stationary phases are considered to be a major breakthrough in separation formats and can be classified into two major groups, which differ in their base chemistry and preparation procedure [1]. Polymeric monolithic stationary phases were introduced in the late 80's and early 90's [2–4]. These materials are based on organic precursors and have, from the very early days, mainly been prepared by free radical initiated (co)polymerization of mono- and di-vinyl precursors in suitable porogenic diluents, in a single-step molding process [5]. This process leads to a typical agglomerated, inter-adhered globule morphology intertwined by micrometer-sized pores. Also, it represents a very efficient and convenient way to prepare stationary phases in the confines of almost any microfluidic conduit size and shape. Therefore these materials are particularly interesting for a broad range of applications in analytical chemistry [6–10]. Due to their single-step preparation by simple liquid molding, the rich variety of options for copolymerization with functional precursors, as well as the ability to introduce required surface functionalities post-polymerization, a wide variety of options to integrate them in micro-analytical devices exists [7,10,11]. The ease of accessibility as porous adsorbent media by thermal, as well as photo-initiated, free radical polymerization is well-recognized and has resulted in many innovative applications. In particular, these materials have proven advantageous for the separation of proteins and (larger) peptides [12–14]. The excellent performance is often explained by the absence of a stagnant mobile phase for large molecules which

do not enter the swollen gel structure of the polymer backbone [3,9,11,15]. Mass transport is therefore assumed to be controlled by convection and remaining contributions to dispersion are that of fluid dispersion in the macropore space [9,16]. Along with this assumption, typical surface areas of these materials range from single m^2/g only for methacrylate-based monoliths [15,17], up to tenths of m^2/g for styrene-based monoliths [18,19]. Therefore, these types of materials are often assumed to perform poorly in the separation of small molecules, particular in isocratic mode [11,18,19].

The second entry of the monolithic materials for chromatography was developed in Tanaka's group in the mid 90's which are based on silica chemistry using inorganic precursors [20,21]. One of the most interesting features is their hierarchical pore structure, which is tailored in a two step process and typically results in total surface areas exceeding 150 m^2/g of up to 370 m^2/g, depending on the preparatory conditions [22,23]. This surface area is realized by a sharp bimodal pore size distribution in the hard silica matter [21,24]. In contrast to polymer-based organic matrices, having a typical agglomerated inter-adhered globule morphology, silica-based monolithic materials consist of a highly porous bicontinuous inorganic skeleton, with a permanent mesoporous pore space (skeletal pores typically in a size range of 2–50 nm) [23]. The excellent combination of high permeability to flow, enabled by micrometer-sized flow-through pores, with that of the desired surface area originating from the skeletal (meso)pores, often enables highly efficient and retention-insensitive performance in the separation of small and medium-sized molecules [22–25]. The often observed excellent and retention-insensitive performance can be explained by the short diffusion distance to and from the active chromatographic sites exposed to the stagnant liquid in the thin skeleton which contains the mesoporous pore space [24]. It further only slightly diminishes at increased flow velocities with typical values of the C-Term of the van Deemter equation well below 10 ms for retained components [25]. This hallmark in performance has not been achieved with that of typical polymer-based monoliths to date [1]. Often plate height curves are constructed with non- or only slightly-retained analytes [25], producing lower C-Terms which we also indicated recently [15]. C-Term values typically exceeding that of 10 ms are observed even under conditions of no retention [25].

The poor performance of typical porous polymer monoliths in the separation of small molecules [9,11,18,19] is often explained by their low surface area and the absence of small pores [19], since that corresponds to the first rational difference in the porous structure of polymer-based and silica-based monoliths, despite morphological considerations [26]. As stated very recently, it has always been difficult to provide a polymeric monolithic material with both macroporous flow-through pores and an array of smaller pores in the actual polymer providing it with the necessary surface area [19]. Methods to increase surface area may include that of post-polymerization hyper-cross-linking reactions which were first pioneered by Davankov and co-workers [27]. They have also been used for hyper-cross-linking of polystyrene bead-based media [28–30] and, recently, monoliths [19]. Hyper-cross-linking can drastically increase surface areas by the presence of micro- and meso-pores persisting even in the dry state [28]. Such polymeric bead-based materials have therefore been envisioned for the separation of small ions due to the predominantly existing micropore sizes in the beads [30].

Another approach to tailor the presence of mesopores focuses on incompletely polymerized monoliths, which was used recently for preparation of monoliths based on styrene chemistry [18,31]. The authors prepared styrene-based monoliths by applying short polymerization times as low as 30–45 min [31]. They further showed that the reduction of the polymerization time results in higher total

porosities and higher permeability in conjunction with the presence of mesoporosity (2–50 nm) and consequently higher specific surface area. The permeability values ranged from 1.29×10^{-14} m^2 to 0.4×10^{-14} m^2 only [31]. We have recently studied the impact of polymerization reaction time on the performance of methacrylate-based macroporous polymer monoliths with more than an order of magnitude higher permeability. Also we found the strongly enhanced performance for monoliths derived from incomplete conversion to be less affected by specific surface areas when studying the isocratic separation of small molecules [15]. Therefore we suggested that the gel porosity, porosity only present in the solvated and swollen polymer [32], becomes the limiting factor for their performance including a retention-dependent efficiency in the separation of small molecules [15]. Such gel-porosity may be ascribed to the presence of varying cross-linking degrees originating from non-ideal reactivity ratios persisting between typically used mono- and di-vinyl precursors in the preparation of macroporous copolymer networks [33]. The resulting polymer network in-homogeneities in their solvated swollen state, irrespective of the presence of already existing small pores, will be detrimental to the separation efficiency. They allow the permeation of small molecules in the nano-scale gel structure and enhance chromatographic dispersion due to stagnant mass transfer resistance in these zones [9,15,34].

In this contribution, we study in depth and explain the key factor for obtaining highly efficient macroporous polymer monoliths derived from a single-step copolymerization preparation. We use an optimized mixture of mono- and di-vinyl precursors with a micro- and macro-porogenic diluent. We initiate polymerization at a relatively low polymerization temperature with a low amount of radical initiator and are, therefore, able to monitor the relatively slow polymerization kinetics. The optimized materials, whose copolymer compositions become readily available from monomer specific conversion studies, contain a permanent mesoporous pore space in conjunction with a minimum amount of gel porosity. The (meso)porous pore space is enabled by the microporogenic diluent in the polymerization precursor mixture. The optimal material allows for separating a homologous series of alkylbenzenes with a retention-insensitive plate height, which only slightly decreases at increased linear mobile phase velocities. Although the approach of incompletely polymerized monoliths was introduced recently [18,31], fluid transport efficiency and retention with small tracers has not been explicitly investigated. Further, the complexity of (co)polymerization kinetics has not been considered in the discussion of the performance of macroporous polymer monoliths in a straightforward way [15].

2. Experimental

2.1. Chemicals and materials

Divinylbenzene (technical grade, 80% mixture of isomers, 20% mainly ethylstyrene), styrene (≥99%), dodecanol, toluene, 3-(trimethoxysilyl)propyl methacrylate, uracil, benzene, alkyl-benzenes and HPLC-grade acetonitrile were purchased from Sigma–Aldrich (Vienna, Austria). Azobisisobutyronitrile (AIBN) was purchased from Fisher Scientific (Vienna, Austria). All monomers were purified over basic alumina to remove the inhibitors. A Millipore Milli-Q Reference water purification system (Vienna, Austria) was used as ultra-pure water source. Uracil, benzene, and alkylbenzenes were dissolved in the mobile phase at typical concentrations of 20 μg/ml uracil and 2 μg/ml each retained analyte. Polyimide-coated fused-silica capillaries of 100 μm I.D. were purchased from Optronis (Kehl, Germany).

2.2. Monolith preparation

The capillaries' inner surface were vinylized as recently reported [8,15] with the exception that 40 wt% 3-(trimethoxysilyl)propyl methacrylate in an ethanolic solution of acetic acid (apparent pH = 5) was used. The optimized precursor mixture for the poly(styrene-*co*-divinylbenzene) monoliths consisted of 24% styrene, 16% divinylbenzene, 42% dodecanol as macroporogen, 18% toluene as microporogen, and 1% AIBN (all w/w). This mixture composition refers to 24% styrene, 12.8% divinylbenzene and 3.2% ethylstyrene (impurity in divinylbenzene) in 40 wt% porogenic diluent (all w/w). It further refers to a ratio of mono- to di-vinyl monomeric precursors typically used for preparation of macroporous polymer scaffolds [8,15]. After deoxygenation of the polymerization mixture with a stream of nitrogen for 5 min, the surface-vinylized capillaries were filled with the precursor mixture using a syringe and were sealed with rubber septa. Polymerization was carried out at 60 °C for variable polymerization times after which the polymerization was effectively quenched by rapid cooling and washing of the polymer with acetonitrile. The defined wash volume of 250 μl from 20 cm long columns was collected for monomer conversion studies with HPLC [15]. The final column length in all experiments was 20 cm.

Bulk polymerizations were carried out in 2 ml glass vials, which were completely filled with the deoxygenated polymerization mixture. Bulk samples were Soxhlet-extracted for 24 h with methanol and dried in a vacuum oven at 40 °C over night. Porous properties were determined via nitrogen adsorption experiments. Monoliths were prepared in duplicate from the same polymerization mixture for these measurements.

2.3. Equipment

Chromatographic measurements were performed on a Dionex Ultimate 3000 nano-LC system (Dionex GmbH, Vienna, Austria) similar to the method described previously [15]. The setup included a 4 nl injection valve switched in line with the flow path and an external UV-detector with a 3 nl internal volume detection cell. Scanning electron micrographs of monoliths in fused-silica capillaries were obtained using a Crossbeam 1540 XB electron microscope (Carl Zeiss SMT AG, Oberkochen, Germany) with a secondary electron detector and the analogous sputtering and detector settings for the different monolithic materials. Nitrogen adsorption experiments were realized with a Micromeritics TriStar Surface area and Porosity Instrument (SY-LAB Geräte GmBH, Neu-Purkersdorf, Austria).

A 1290 Infinity UHPLC system (Agilent Technologies, Vienna, Austria) equipped with a diode array detector and a Zorbax Eclipse Plus C18 column (2.1 mm × 50 mm, packed with 1.8 μm particles) was used for monomer conversion studies. UV-detection was carried out at 254 nm and peak areas allowed calculation of remaining monomer after termination of the polymerization reaction. For that purpose the defined volume of eluate from washing 20 cm long capillaries with acetonitrile (250 μL) was collected, diluted with running mobile phase of the UHPLC system and injection of 20 μl was performed under identical conditions for all diluted eluate samples. The isocratic separation of styrene, divinylbenzene and ethylstyrene (20% impurity in divinylbenzene) in isocratic mode, as well as linearity of detector response allowed determination of monomer specific conversion.

3. Results and discussion

Macroporous polymer monoliths are almost exclusively derived from copolymerization reactions though there seems a recent trend in deriving them from homopolymerizations of multi-vinyl monomers. This is due to suggested repeatability issues and structural properties including higher cross-linking degrees and surface areas [35–37]. However, copolymerization is often required to introduce the desired functionality in the macroporous polymer monolith scaffold and provide their external surface with interacting moieties or provide it with the desired reactive functionality which allows post-polymerization modification of the material [38]. By default this also may result in phase-separated polymer network in-homogeneities due to the different reactivity ratios persisting between typically used mono- and di-vinyl monomeric precursors [15,33,39]. Since a commonly employed divinyl monomer shows higher reactivity than typically used monovinyl precursors, the resulting copolymerization may be a complicated process. It includes the complexity arising from nucleation and globule formation, phase separation and completion of the polymerization reaction.

Initial screening experiments with our precursor mixture show a polymer phase separation with coalescence and rigid, wall-adhered macroporous polymer after a polymerization time of 3 h. This relatively long time for phase separation and 3D coalescence is untypical for styrene-based [31] and methacrylate-based polymer monoliths [15]. It is caused by the relatively low initiator concentration, polymerization temperature and the slower reaction kinetics of styrene-based monomers in comparison to e.g. methacrylates [40]. However, these conditions were deliberately chosen to allow convenient termination of the polymerization reaction. In order to understand the most important parameters of the porous polymer monoliths performance, we decided to design complementary experiments. These experiments included monomer specific conversion in the capillary-sized mold, surface area measurements from bulk preparations, microscopic investigations, and study of porous and hydrodynamic properties through their final performance in the isocratic separation of small molecules.

3.1. Monomer conversion

In order to understand the copolymerization dynamics in our 100 μm I.D. sized mold, we investigated the monomer specific conversion focusing on the main constituents of the polymerization mixture composed of styrene, divinylbenzene, and minor constituent ethylstyrene in the porogenic diluent (Fig. 1). At a polymerization time of 3 h, i.e. soon after phase separation, 50% of the original amount divinylbenzene is converted to the polymeric stationary phase, while only 29% of monovinyl monomer styrene (and similar amount ethylstyrene) has reacted. Consequently, the relative amount of cross-linker in the non-polymerized mixture is significantly lower after 3 h of polymerization [33]. This is directly observed in the higher monomer specific conversion of divinylbenzene in the early stages of the polymerization reaction and indicates a high degree of cross-linking in the polymer scaffold [15,33]. In other words, the molecular composition of the scaffold at this stage of the polymerization reaction consists of a ratio of mono- to di-vinyl monomers close to 1:1.2 at an overall total conversion of 36%. Longer polymerization time leads to further rise in conversion of mono-vinyl monomeric precursors as the remainder of the polymerization mixture is depleted of di-vinyl monomer (Fig. 1). Conversion of divinylbenzene remains higher than that of mono-vinyl monomer styrene (and impurity ethylbenzene) and therefore reaches completeness faster than that of the mono-vinyl monomers (Fig. 1). These results demonstrate the development of a heterogeneous copolymer network structure which shows a cross-link density distribution [15,33]. It results in a less densely cross-linked polymer being formed in later stages of the polymerization reaction (longer than 3 h) and being attached to a more cross-linked underlying polymer structure. The presence of less cross-linked
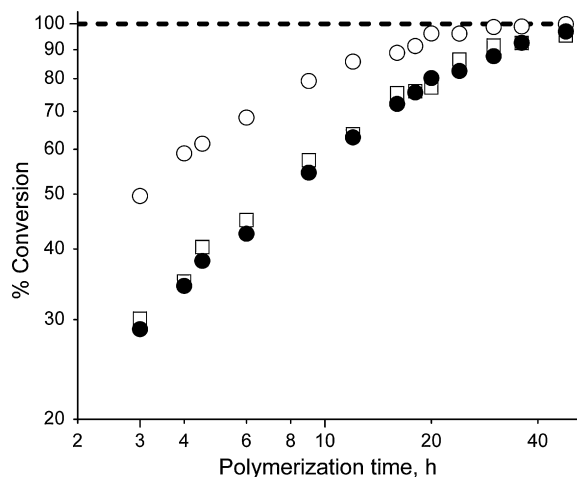
Fig. 1. Monomer specific conversion of styrene (●), ethylstyrene (□) and divinylbenzene (○) in 100 μm I.D., previously vinylized, fused-silica capillaries obtained at variable polymerization times after which the reaction was terminated. Remaining monomer content was determined by HPLC analysis of a defined wash volume eluted from the capillaries with acetonitrile (see Section 2). Three hours polymerization time correspond to that after phase separation where a pressure stable porous polymer was obtained.

polymer in styrene-based polymer beads and its elucidation was published as early as 1985 [32] confirming these anticipations. Completion of the polymerization reaction with a total conversion approaching a 100% for styrene (and ethylstyrene) is possible only at polymerization times of 48 h (see dashed line in Fig. 1 for a 100% conversion). However, the amount of divinylbenzene for further cross-linking already approaches zero at polymerization times of 18–25 h.

3.2. Nitrogen adsorption experiments

The cumulative pore volume data of identical polymerization mixtures polymerized in 2 ml glass vials and at variable polymerization times are shown in Fig. 2. These measurements were each performed for two prepared monoliths, properly dried and consequently in their non-swollen state. After 3 h polymerization time (the minimum reaction time at which a pressure stable wall-ad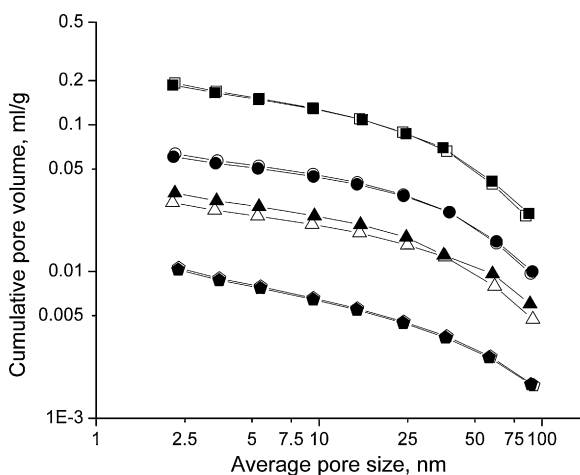hered monolith in the capillaries was formed), the total volume of pores between 2 and 100 nm average pore sizes reaches a value close to 0.2 ml/g. This pore volume indicates a significant amount of a permanent porosity inside the globules. It stems from the microporogen toluene of 18 wt% (equal to 20.8 vol.%) in the polymerization mixture. An increased polymerization time decreases this pore volume by more than an order of magnitude to 0.01 ml/g at 48 h. The corresponding cumulative pore volume of this material corresponds to a surface area of only 5–6 m^2/g, while it approaches a 100 m^2/g at a polymerization time of 3 h. This is similar to what has been found previously for macroporous styrene-based monoliths in the work of Trojer et al. [31]. However, due to our lower polymerization temperature and AIBN concentration much slower polymerization kinetics are observed in the current study.

3.3. Microscopic properties

Fig. 3 shows the morphology of the polymer monoliths in a 100 μm I.D. fused-silica capillary, shortly after phase separation at a polymerization time of 3 h (50% divinyl monomer conversion, 29–30% monovinyl monomer conversion, see Fig. 1) and after 48 h resulting in near completion of the polymerization reaction (>99% divinyl monomer conversion, >95% monovinyl monomer conversion, see Fig. 1). The macroporous inter-adhered globule structure is evident, as well as the fine porous structure at a polymerization time of only 3 h (Fig. 3a, right hand side). Indeed the globule-scale morphology shows larger clusters, which are clearly featured by small pores in the tenth of nanometer range (including mesopores of 2–50 nm). This finer structure on a nanometer scale is responsible for the higher pore volume determined by nitrogen adsorption (Fig. 2). It indicates certain features of hierarchy with intra-globular pores in the tenth of nanometer range and micrometer-sized inter-globular pores (Fig. 3a, left hand side). This agrees well with the nitrogen adsorption data which clearly confirm a significant rise in pore volume between 10 and 100 nm sized pores at incomplete conversion. Further, it is indicated that this polymer material has a higher degree of cross-linking than polymer formed in later stages of the polymerization reaction (Fig. 1). At increased polymerization time, the smaller voids inside the globules are filled with the remaining polymerizing monomers (they are good "solvent" for the phase separated polymer [41]). This also leads to a globule growth with an overall lower degree of cross-linking (Fig. 1) [15]. The effective filling of the small pores corresponds with the nitrogen adsorption data (e.g. Fig. 2, 48 h polymerization time) as well as SEM images (Fig. 3b). The corresponding SEM image at 48 h polymerization time (Fig. 3b, right hand side) shows a globular structure with the apparent absence of small pores in the dry state and consequently low pore volumes and surface areas (Fig. 2).

3.4. Porosity and permeability

We used two approaches to estimate the total porosity, ε_t, of the monoliths in dependence of polymerization reaction time. First, it is a well-known fact that the porosity of porous polymer monoliths is related to the ratio of monomeric precursor to porogenic diluent. This simple rational does not take into account the volume-shrinkage typical of all free radical polymerizations [8]. Since the ratio of monomeric precursor to porogenic diluent from the precursor mixture is known, our conversion studies in Fig. 1 readily allow estimation of ε_t of the scaffold excluding volume-shrinkage. The volume-amount of polymer was simply estimated by the sum of the products of the volume fractions (derived from the weight fractions) of each monomer with its conversion. Subsequently, the obtained value was subtracted from a 100%, resulting in a theoretical estimate of ε_t in our 100 μm I.D.-sized mold. On the other hand,

Fig. 2. Cumulative pore volume data of poly(styrene-co-divinylbenzene) monoliths prepared in 2 ml HPLC vials at different polymerization times, determined by nitrogen adsorption. Each polymer was prepared two times from the same polymerization mixture, indicated by open and closed symbols. Symbols: 3 h (squares), 6 h (circles), 9 h (triangles), and 48 h (pentagons).

ε_t was determined via nano-LC experiments (with uracil assumed to sample all available pore space in the porous structure and being non-retained) [8,15].

The results of these estimates are shown in Fig. 4a. Both values (see open and closed symbols) show a consistent decrease at increased polymerization times. We observe higher values of the porosity determined by nano-LC. This may be explained by the volume shrinkage typical for free-radical polymerizations [8]. However, a scaffold derived from 3 h polymerization time (total conversion = 36%), with a porosity determined by nano-LC near to a 90%, has the highest amount of divinyl monomer available for potential cross-linking reactions in the formed polymer (Fig. 1). In contrast at 48 h polymerization time, the determined porosity of 61% indicates a close to total conversion of monomeric precursors (total conversion = 97.7%, Fig. 1). The total porosity of close to 60% at almost complete conversion therefore reflects the ratio of monomer to porogenic diluent in the original polymerization mixture [8], which is in our case 56% (see dashed line in Fig. 4a). The remaining difference between both ways of determination stems from volume shrinkage.

The superficial velocity-based hydrodynamic permeability, $k_{p,f}$, decreases significantly at increased polymerization times (Fig. 4b). The significant decrease in permeability indicates the absolute growth of globules in due course of the proceeding polymerization reactions, thus decreasing the average macropore size in the porous structure. This is in conjunction with an effective filling of the smaller cavities in the globule clusters (Fig. 3). To measure the rigidity of the polymer backbone for the lowest and highest polymerization times, Fig. 5 shows a plot of backpressure against applied flow rate for two prepared columns at each polymerization time. Fig. 5 confirms linearity of the slope of backpressure for the monoliths. It also demonstrates that the porous structure does not become compressed up to the maximum flow rates. For example, a flow rate of 2 μl/min translates to a back pressure of 40 MPa/m for a monolith derived from 3 h polymerization time. Accordingly, a monolith derived from a 48 h polymerization time, shows more than three times higher back pressure.

3.5. Isocratic performance

Fig. 6 shows the separation of a homologous series of alkylbenzenes at a similar linear chromatographic flow velocity for monoliths obtained after polymerization times of 3 and 48 h, respectively. This was realized by proper adjustments in flow rate due to varying porosities found in Fig. 4a. These columns correspond to the SEM images shown in Fig. 3. The high peak width of the retained components for a completely polymerized material is apparent (Fig. 6b and Fig. 3b) while it is much narrower for a material polymerized for 3 h (Fig. 6a and Fig. 3a). The narrower elution width in Fig. 6a can directly be related to the existence of a permanent (meso)porous pore space (Figs. 2 and 3a), a higher porosity (Fig. 4a) and a highly cross-linked lower amount of polymer material in which the analytes distribute (Fig. 1). However, the increased retention of alkylbenzenes for a monolith at complete conversion (Fig. 6b) with a much lower (meso)pore volume and consequently surface area in their dry state (Figs. 2 and 3) indicates the accessibility of the swollen gel-structure with hampered mass transfer efficiency in nano-LC (Fig. 6b). The solvated and swollen polymer globs allow the permeation of small molecules, thus resulting in an increased retention. We have observed a similar effect for methacrylate-based macroporous polymer monoliths despite their significantly lower surface area and higher permeability [15]. This becomes evident by the absolute amount of polymer material inside the capillary and related retention. For example, based on our conversion (Fig. 1) and porosity results (Fig. 4a) representing the amount of polymer in the capillary, we find a retention factor spanning $k' = 0.59$ to $k' = 3.3$ for a total conversion of 36% and overall 90% measured column porosity (Fig. 4a and Fig. 6a). In turn for a near-total conversion (total conversion = 97.7%, Fig. 1) resulting in an overall 61% measured column porosity (Fig. 4a), a retention factor of $k' = 2$ to $k' = 11.3$ is obtained (Fig. 6b). This corresponds to a factor of 3.4. Therefore it is safe to assume that the small hydrophobic tracers penetrate the styrene-*co*-divinylbenzene matrix irrespective of indication of significant amount of small pores in their dry state (Figs. 2 and 3). This obser-
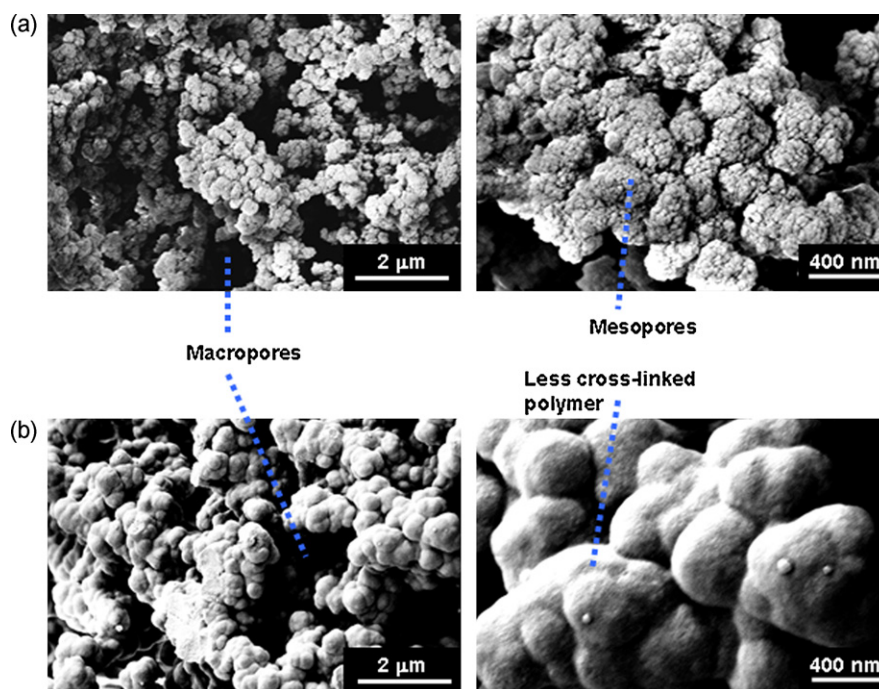

Fig. 3. Scanning electron micrographs of the porous monolithic poly(styrene-*co*-divinylbenzene) columns prepared in 100 μm I.D. fused-silica capillaries obtained after (a) a polymerization time of 3 h and (b) a polymerization time of 48 h. Two different magnifications are shown.
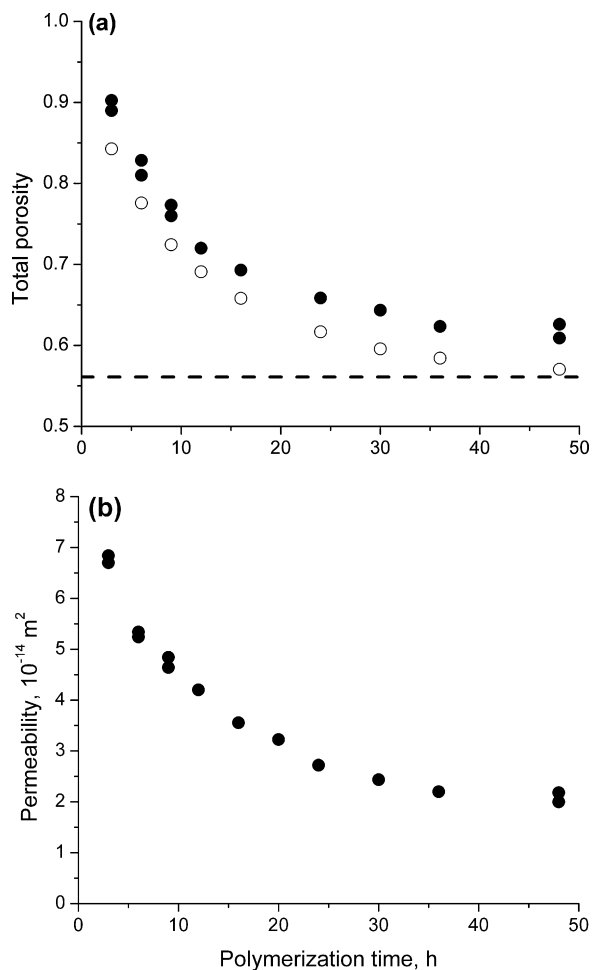
Fig. 4. Porous and hydrodynamic properties of monolithic poly(styrene-*co*-divinylbenzene) columns in the confines of a 100 μm I.D. capillary elucidated by nano-LC, in dependence of polymerization reaction time. Mobile phase: 70% (v/v) acetonitrile in water. (a) Total porosity, ε_t, measured with uracil as non-retained, totally permeating solute in nano-LC (●) [8,15], and derived from the monomer specific conversion in Fig. 1 (○). (b) Superficial velocity-based hydrodynamic permeability $k_{p,f}$ [8,15].
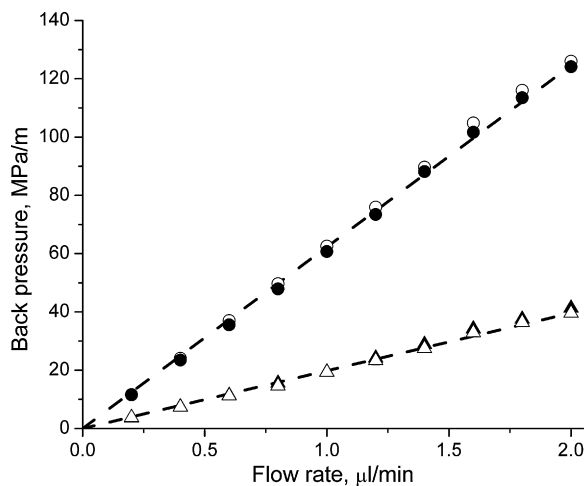
Fig. 5. Back pressure of monolithic poly(styrene-*co*-divinylbenzene) columns against applied flow rate for selected polymerization times of 3 h (triangles) and 48 h (circles). Two prepared columns at the respective polymerization time are shown by open and closed symbols. Mobile phase: 70% (v/v) acetonitrile in water.
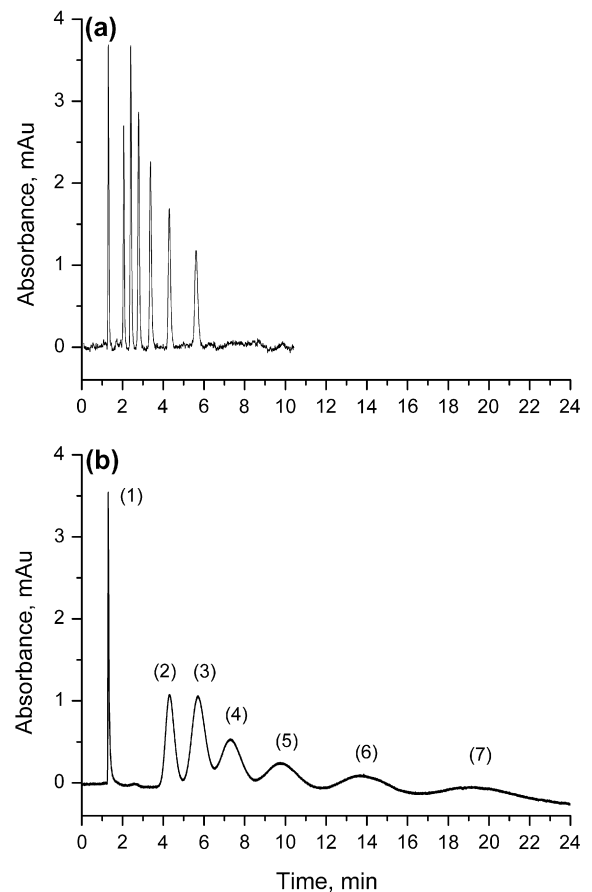

Fig. 6. Separation of alkylbenzenes on porous monolithic poly(styrene-*co*-divinylbenzene) columns in a 100 μm I.D. capillary obtained after different polymerization times. (a) Monolith obtained after a polymerization time of 3 h. (b) Monolith obtained after a polymerization time of 48 h. Conditions: isocratic elution. Similar linear chromatographic velocity of $u_0 = 2.5$ mm/s. Mobile phase: 70% (v/v) acetonitrile in water. Injection volume: 4 nl. Peaks: (1) uracil, (2) benzene, (3) toluene, (4) ethylbenzene, (5) propylbenzene, (6) butylbenzene, and (7) pentylbenzene.

vation is congruent to that made more than 20 years ago for their bead-based counterpart [34].

Both monoliths shown in Fig. 6 show a similar selectivity in the separation of alkylbenzenes. This becomes clear from the plot of retention against number of alkyl carbon atoms for both materials in Fig. 7. The result is similar for methacrylate-based macroporous polymer monoliths despite its faster polymerization kinetics, overall lower surface area, higher permeability, and lower methylene selectivity [15]. The higher mesopore volume and consequently surface area obtained at shortened polymerization times (Fig. 2) does not increase retention neither does it increase selectivity in the separation of alkylbenzenes (Fig. 7). This becomes clear by the similar slope of both curves shifted by a constant value of a factor of 3.4 in Fig. 7. This most important result clearly contrasts widely made assumptions that high surface areas and mesopore volumes are required for the efficient separation of small molecules for polymer-based monolithic columns [9,11,19]. Due to hampered mass transfer in the gel structure (representing the actual swollen polymer) at complete polymerization (Fig. 3b), the retained analytes appear unacceptably broad with the last eluting component pentylbenzene showing highest dispersion (Fig. 6b). The efficiency significantly drops with increased elution time, i.e. retention [15], while it appears similar for all tracers with a monolith obtained from a short polymerization time (Fig. 6a).
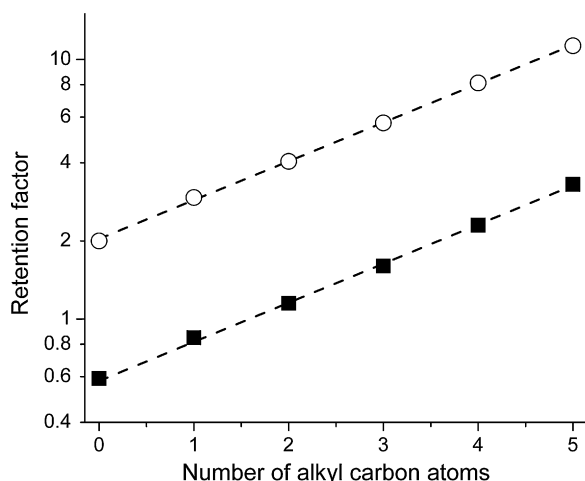
Fig. 7. Retention of alkylbenzenes against number of alkyl carbon atoms on mono-lithic poly(styrene-*co*-divinylbenzene) columns obtained after 3 h (■) and 48 h (○) polymerization time, respectively. Same chromatographic conditions as in Fig. 6.

Fig. 8 demonstrates the performance of the monoliths obtained after 3 h polymerization time, for two different chromatographic flow velocities, at the medium and maximum of flow speed used in this work. Clearly a baseline separation of all tracers with high selectivity and resolution becomes possible even at a linear chromatographic velocity of 4.5 mm/s (upper trace and inset in Fig. 8). It allows the isocratic separation of structurally related compounds differing in just one methylene unit. Still there is room for additional peak capacity. Fig. 9 demonstrates the excellent retention-insensitive performance for all five alkylbenzenes spanning retention factors from $k' = 0.59$ to a $k' = 3.3$. This condition is usually encountered with typical silica-based materials [25] and contrasts that of methacrylate-based porous polymer monoliths [15,42]. All plate height curves in this retention range lead to one single master curve.
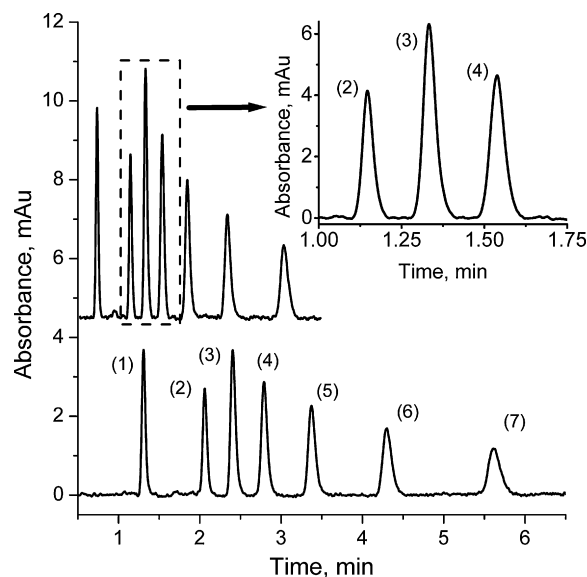

Fig. 8. Separation of uracil, benzene and five alkylbenzenes at a linear chromato-graphic velocity of $u_0 = 2.5$ mm/s (lower trace) and $u_0 = 4.5$ mm/s (upper trace) as well as efficient isocratic resolution of benzene, toluene, and ethylbenzene (see inset) using a poly(styrene-*co*-divinylbenzene) monolithic column obtained after 3 h polymerization time. Elution order and peak assignment is the same as in Fig. 6. Mobile phase: 70% (v/v) acetonitrile in water.
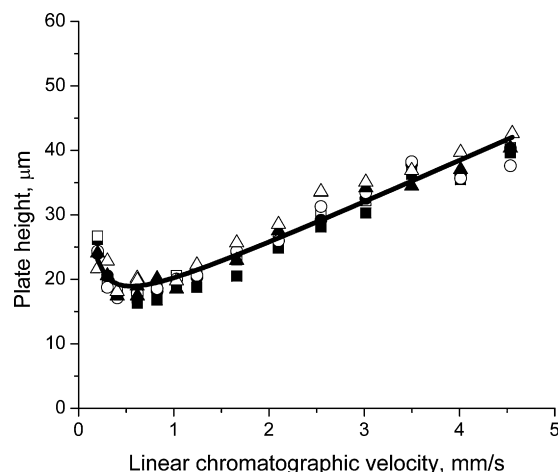

Fig. 9. Plate height curves obtained from separations on a monolithic poly(styrene-*co*-divinylbenzene) column obtained after 3 h polymerization time for retained tracers benzene (■), toluene (□), ethylbenzene (●), propylbenzene (○), butyl-benzene (▲), and pentylbenzene (△), respectively, showing insensitivity of the performance on chromatographic retention for retention factors ranging from $k' = 0.59$ to a $k' = 3.3$ (Fig. 7). Mobile phase: 70% (v/v) acetonitrile in water. The plate heights for butylbenzene were fitted to the van Deemter equation $H = A + B/u + Cu$, shown by the solid line.
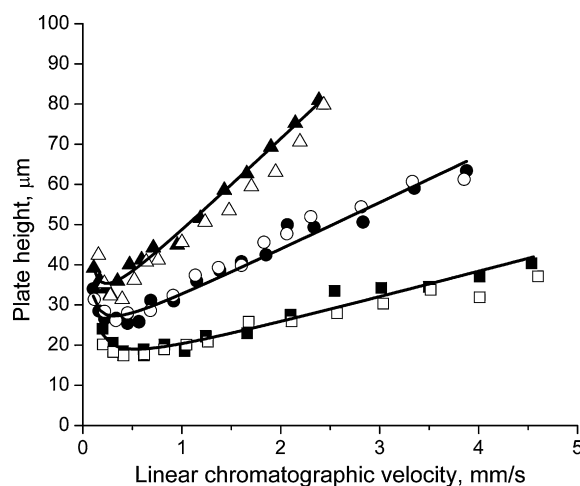

Fig. 10. Impact of polymerization time on plate height curves for butylbenzene eluted on monolithic poly(styrene-*co*-divinylbenzene) columns. Symbols: 3 h poly-merization time (squares) with a $k' = 2.3$, 6 h polymerization time (circles) with a $k' = 4.5$, and 9 h polymerization time (triangles) with a $k' = 6$. Mobile phase: 70% (v/v) of acetonitrile in water. Two prepared columns each were investigated indicated by closed and open symbols. Van Deemter fit $H = A + B/u + Cu$ shown by the solid lines.

3.6. Impact of polymerization time on height equivalent to a theoretical plate

We used the van Deemter model introduced more than 50 years ago [43] and still being considered as a reliable model for description of chromatographic processes [44] to evaluate our column performance. To interpret the performance of our monoliths we recorded plate height curves for butylbenzene, which shows significant retention on all stationary phases (Fig. 7). Fig. 10 shows the plate height curves of retained butylbenzene using monoliths derived from polymerization times of 3, 6 and 9 h. Two prepared monoliths (see filled and open symbols) are shown at the respective polymerization times. It is apparent that the plate height is lowest at a minimum polymerization time of 3 h with a minimum plate height between 15 and 20 μm. These columns have a total porosity of 90% (Fig. 4a), a composition of mono and

di-vinyl monomer 1:1.2 and therefore a polymer backbone with a high degree of cross-linking at an overall conversion of 36% (Fig. 1). Further they have the highest pore volume of smaller 100 nm sized pores from all materials investigated (Fig. 2). At increased linear flow velocity we see an increase in plate height with a C-Term of 6.5 ms, slightly higher to the range of typical silica-based monoliths as reviewed by Siouffi [25].

Increased polymerization times show a significant increase in plate height with an apparently stronger increase of the plate height with mobile phase velocity. Another interesting aspect arising from these curves is the shift of the minimum plate height to lower linear chromatographic velocities. The C-Term describing mass transfer resistance in the chromatographic process starts to dominate over the whole flow velocity range. The initial C-Term of 6.6 ms after 3 h polymerization time increases subsequently to 11.8 ms and 23.3 ms at 6 and 9 h polymerization time, respectively. At polymerization times higher 9 h (total conversion > 62.7%, Fig. 1) plate heights become unacceptable and did not make much sense to show in Fig. 10.

The decrease in performance at increased polymerization times in Fig. 10 is caused by the increased importance of mass transfer resistance which may originate from stagnant mass transfer zones in the porous structure [15]. This mass transfer resistance may be caused by more slightly cross-linked polymer which allows permeation of small molecules when it is solvated and swollen by the mobile phase [32,34]. It also explains the strong polymerization time-dependency of methacrylate-based macroporous polymer monoliths' performance we observed recently [15]. Under this condition the increased surface area at a terminated polymerization reaction just appears to be a 'side-effect' in reduction of potential polymer mass in which the analytes distribute. The increased importance of the mass transfer term is evident, in particular for a lower surface area material. The increased mass transfer resistance determines the plate height almost across the whole linear chromatographic velocity at increased polymerization times (Fig. 10).

At a relatively short polymerization time of 3 h our results indicate the possibility of the preparation of high permeability, pressure-stable monoliths (Figs. 4a and 5) with a retention-insensitive plate height (Fig. 9). This retention-insensitive performance can be understood by our monomer conversion studies (Fig. 1), porosity (Fig. 4a), permeability (Fig. 4b), and nitrogen adsorption data (Fig. 2). For example, at 3 h polymerization time a highly cross-linked scaffold with a permanent mesoporous pore space is obtained, which, due to a proceeding polymerization reaction loses its mesoporosity because the pores and surroundings of initially phase-separated globules are softened with more slightly cross-linked polymer (Figs. 1 and 3). This polymer allows the permeation of small molecules in nano-LC, since we see an increased retention (phase ratio) and also dispersion with increased polymerization times (Figs. 6 and 7). This result also shows the detrimental effect of the more slightly cross-linked polymer gel on the isocratic performance in the separation of small molecules.

With respect to these reported results it becomes evident that the soft matter columns prepared in this work allow for an optimum efficiency at a maximum porosity in the studied system (Fig. 4a), a maximum amount of (meso)pore volume (Fig. 2), and a maximum in permeability (Fig. 4b). All these properties are realized by a minimum of highly cross-linked polymer mass in the confine itself (Fig. 1) allowing for retention, selectivity and most importantly a minimum of band broadening.

4. Conclusions

We have demonstrated and explained, how through careful adjustment of polymerization time and understanding dynamics of copolymerization, macroporous poly(styrene-co-divinylbenzene) monoliths with a highly efficient isocratic and retention-insensitive performance in the separation of small molecules can be prepared. Though it appears tempting to attribute the enhanced performance to the existence of a permanent mesoporous pore space and consequently relatively high surface area, our experiments clearly confirm another important aspect in the performance of these monoliths. The enhanced performance of monoliths with a given base-chemistry is always achieved at an overall lower capacity factor (retention factor). This is due to an overall lower amount of polymeric mass in the confine showing a varying degree of cross-link density and consequently gel porosity, which again results from swelling. This most important result clearly contrasts widely made assumptions that high surface areas and mesopore volumes are required for the efficient separation of small molecules. The increased surface area was shown to be just a 'side-effect' resulting from the reduction of gel-porosity. Again this gel porosity is absent in the dry state of the polymer. This influence became accessible only by carefully designed isocratic experiments where the residence time of the tracer is not controlled by a mobile phase gradient. It was confirmed by independent measurements using nitrogen adsorption, electron microscopy, monomer specific conversion in the capillary, permeability as well as porosity measurements. We further correlated these results with the final isocratic separation of small retained tracers enabling generation of plate height curves for tracers spanning significant ranges of retention factors exceeding a k' of 3.

The existence of a minimum amount of polymer showing gel porosity and consequently a permanent (meso)porous globule structure was demonstrated to aid small molecule separation with a retention-insensitive performance over a wide range of retention-factors and chromatographic flow velocity. Though only probed for typical alkylbenzenes it is anticipated that these materials will prove suitable for the efficient separation of a wider range of small analytes. In that line, the major limiting factor of their performance arises from the flow heterogeneity in the macroporous pore space, which may be improved by more controlled chain growth, cross-linking, and phase separation. Therefore, ongoing experiments are suggested clarifying the actual double bond conversion in the scaffold shortly after phase separation with that in the more slightly cross-linked outer regions of the globular structures as this understanding would shed more light on possible manipulation strategies of the nano-scale polymer structure and microscale heterogeneity of the scaffold.

Acknowledgements

References

[1] G. Guiochon, J. Chromatogr. A 1168 (2007) 101.
[2] S. Hjertén, J.L. Liao, R. Zhang, J. Chromatogr. 473 (1989) 273.
[3] F. Svec, J.M.J. Fréchet, Anal. Chem. 64 (1992) 820.
[4] Q.C. Wang, F. Svec, J.M.J. Fréchet, Anal. Chem. 65 (1993) 2243.
[5] F. Svec, T.B. Tennikova, Z. Deyl, Monolithic Materials: Preparation, Properties, and Applications, Elsevier, Amsterdam, 2003.
[6] K.W. Ro, R. Nayalk, D.R. Knapp, Electrophoresis 27 (2006) 3547.
[7] T.C. Logan, D.S. Clark, T.B. Stachowiak, F. Svec, J.M.J. Fréchet, Anal. Chem. 79 (2007) 6592.
[8] I. Nischang, F. Svec, J.M.J. Fréchet, J. Chromatogr. A 1216 (2009) 2355.
[9] I. Nischang, O. Brüggemann, F. Svec, Anal. Bioanal. Chem. 397 (2010) 953.

[10] J.K. Liu, C.F. Chen, C.W. Tsao, C.C. Chang, C.C. Chu, D.L. Devoe, Anal. Chem. 81 (2009) 2545.
[11] F. Svec, J. Chromatogr. A 1217 (2010) 902.
[12] I. Gusev, X. Huang, C. Horvath, J. Chromatogr. A 855 (1999) 273.
[13] A. Premstaller, H. Oberacher, C.G. Huber, Anal. Chem. 72 (2000) 4386.
[14] A.R. Ivanov, L. Zang, B.L. Karger, Anal. Chem. 75 (2003) 5306.
[15] I. Nischang, O. Brüggemann, J. Chromatogr. A 1217 (2010) 5389.
[16] A. Jungbauer, R. Hahn, J. Sep. Sci. 27 (2004) 767.
[17] Z.D. Xu, L.M. Yang, Q.Q. Wang, J. Chromatogr. A 1216 (2009) 3098.
[18] A. Greiderer, L. Trojer, C.W. Huck, G.K. Bonn, J. Chromatogr. A 1216 (2009) 7747.
[19] J. Urban, F. Svec, J.M.J. Fréchet, Anal. Chem. 82 (2010) 1621.
[20] H. Minakuchi, K. Nakanishi, N. Soga, N. Ishizuka, N. Tanaka, Anal. Chem. 68 (1996) 3498.
[21] K. Nakanishi, H. Minakuchi, N. Soga, N. Tanaka, J. Sol–Gel Sci. Technol. 8 (1997) 547.
[22] N. Tanaka, H. Nagayama, H. Kobayashi, T. Ikegami, K. Hosoya, N. Ishizuka, H. Minakuchi, K. Nakanishi, K. Cabrera, D. Lubda, J. High Resol. Chromatogr. 23 (2000) 111.
[23] N. Tanaka, H. Kobayashi, K. Nakanishi, H. Minakuchi, N. Ishizuka, Anal. Chem. 73 (2001) 420A.
[24] U. Tallarek, F.C. Leinweber, A. Seidel-Morgenstern, Chem. Eng. Technol. 25 (2002) 1177.
[25] A.M. Siouffi, J. Chromatogr. A 1126 (2006) 86.
[26] H. Aoki, N. Tanaka, T. Kub, K. Hosoya, J. Sep. Sci. 32 (2009) 341.
[27] M.P. Tsyurupa, L.A. Maslova, A.I. Andreeva, T.A. Mrachkovskaya, V.A. Davankov, React. Polym. 95 (1995) 69.
[28] N.A. Penner, P.N. Nesterenko, M.M. Ilyin, M.P. Tsyurupa, V.A. Davankov, Chromatographia 50 (1999) 611.
[29] V.A. Davankov, M. Tsyurupa, M. Ilyin, L. Pavlova, J. Chromatogr. A 965 (2002) 65.
[30] V. Davankov, M.M. Tsyurupa, J. Chromatogr. A 1087 (2005) 3.
[31] L. Trojer, C.P. Bisjak, W. Wieder, G.K. Bonn, J. Chromatogr. A 1216 (2009) 6303.
[32] K. Jerabek, Anal. Chem. 57 (1985) 1598.
[33] O. Okay, Prog. Polym. Sci. 25 (2000) 711.
[34] F. Nevejans, M. Verzele, J. Chromatogr. 406 (1987) 325.
[35] S.H. Lubbad, M.R. Buchmeiser, J. Sep. Sci. 32 (2009) 2521.
[36] S.H. Lubbad, M.R. Buchmeiser, J. Chromatogr. A 1217 (2010) 3223.
[37] Y. Li, H.D. Tolley, M.L. Lee, J. Chromatogr. A 1217 (2010) 4934.
[38] F. Svec, LC-GC Europe 23 (2010) 272.
[39] H.J. Naghash, O. Okay, Polymer 38 (1997) 1187.
[40] K.C. Berger, G. Meyerhoff, in: J. Brandrup, E.H. Immergut (Eds.), Polymer Handbook, 4th ed., Wiley, New York, 1989.
[41] F. Svec, J.M.J. Fréchet, Chem. Mater. 7 (1995) 707.
[42] Y. Huo, P.J. Schoenmakers, W.T. Kok, J. Chromatogr. A 1175 (2007) 81.
[43] J.J. van Deemter, F.J. Zuiderweg, A. Klinkenberg, Chem. Eng. Sci. 5 (1956) 271.
[44] K.M. Usher, C.R. Simmons, J.G. Dorsey, J. Chromatogr. A 1200 (2008) 122.